

# Validity of use of a Fabry—Perot interferometer in a Raman scattering lidar

S.N. Volkov

*Institute of Atmospheric Optics,  
Siberian Branch of the Russian Academy of Sciences, Tomsk*  
Received December 15, 1998

In this paper I propose a new design of a monochromator utilizing the autocollimator optical arrangement. It includes a Fabry—Perot interferometer and a diffraction grating. The validity of the design proposed is analyzed.

Requirements imposed upon sensing instrumentation, such as high resolution, small size, and stability of the performance parameters, initiate searching for new, and more efficient design. The Fabry-Perot interferometer (FPI) attracts considerable interest as far as concerned its application to separation of narrow spectral regions in laser sensing based on Raman light scattering (RS).<sup>1-3</sup> FPI has been noted as ensuring reliable separation of the RS rotational structure of atmospheric oxygen and nitrogen, thus allowing determination of temperature profiles in the atmosphere with a Raman lidar. It has been shown<sup>4</sup> that the optimal solution to this problem is to separate two lines, for example, with quantum numbers of 6 and 14, from the pure rotational Raman spectrum of nitrogen. The optimal instrumental solution for such a separation is to use a Fabry-Perot interferometer coupled with a diffraction grating. In such a design, the interferometer is set, as shown in Fig. 1, into the lens—grating optical arm of the diffraction monochromator utilizing the autocollimator scheme.

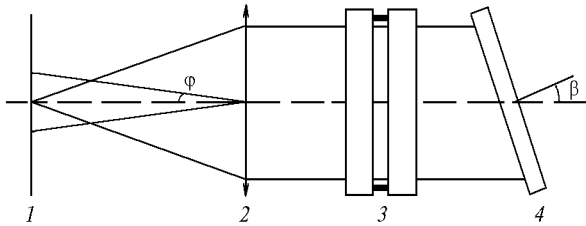


**Fig. 1.** Arrangement of the proposed monochromator: the monochromator entrance/exit plane (1); a lens (2); a Fabry—Perot interferometer (3); a diffraction grating (4).

The monochromator employs the following principle of operation.

Figure 2 shows the arrangement of entrance and exit slits for the case of monochromator matched with the round apertures. The exit apertures 2 and 4 serve for isolation of the lines with the rotational quantum numbers of 6 and 14, respectively, from the Stokes and anti-Stokes wings of the purely rotational Raman spectrum of nitrogen. The aperture 3 collects the on-line scattered radiation attenuated while two times passing through the instrument.

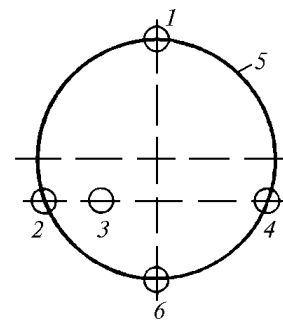


**Fig. 2.** Position of the round apertures on the receiving plane: the entrance aperture (1); the exit apertures (2, 3, 4, and 6); a circle passing through the entrance and exit apertures (5).

A non-attenuated radiation at the sensing wavelength is directed to the exit aperture 6 reflected from the interferometer backward as a result of interference. The circular entrance/exit arrangement, symmetrical about the monochromator optical axis, is used. As a result, if light guides are placed on the circle 5, the conditions for interference in the Fabry—Perot interferometer are identical

$$2 d \mu \cos \varphi = m \lambda , \quad (1)$$

where  $d$  is the distance between the interferometer plates;  $\varphi$  is the angle of wave front incidence onto the interferometer;  $m$  is the order of interference pattern;  $\mu$  is the refractive index;  $\lambda$  is the wavelength.

Upon passage through the entrance aperture 1, the radiation comes to the lens. Then it is incident, as almost a plane wave, on the interferometer at an angle  $\varphi$ . The separation between interferometer plates is chosen so that the spectral selection made by the interferometer corresponds to pure rotational Raman spectrum of nitrogen<sup>5</sup> with a step of  $7.958 \text{ cm}^{-1}$ .

Once passing through the interferometer, the radiation comes to the diffraction grating, where the spectral selection occurs. The grating is adjusted so that radiation at the two wavelengths, corresponding to the rotational quantum numbers of 6 and 14, was incident back onto the interferometer at an angle  $\varphi$ . The radiation selected twice by the interferometer is focused by the lens onto the exit apertures 2 and 4.

Note, that if a plane mirror is used instead of a grating and the mirror is adjusted so that the reflected radiation is incident onto the interferometer at an angle  $\varphi$ , then the pattern for the intensity envelope, formed behind the lens at the image plane, is similar to the pattern of diffraction on a circular opening with the effective cross section equal to the input aperture of the opening. With the diffraction grating, the pattern across the plane of angular spectral selection of the grating remains unchanged.

Such parameters as the relative opening of the matched optical system  $O$ , the entrance/exit apertures  $A_c$  and the aperture of the Fabry–Perot interferometer  $A_{\text{FPI}}$ , as well as the angle of diffraction  $\beta$ , are used as the initial known data in our calculations.

Then the focal length of the lens  $F$  can be determined as

$$F = A_{\text{FPI}}^* O . \quad (2)$$

The reciprocal linear dispersion  $D_{\text{lin}}$  is calculated by the expression

$$D_{\text{lin}} = \lambda / (2F \tan \beta) . \quad (3)$$

The parameters of the Fabry–Perot interferometer are determined in the following way:

$$\delta m = (1 - R) / (\pi \sqrt{R}) ; \quad (4)$$

$$K_i = [(1 + R) / (1 - R)]^2 ; \quad (5)$$

$$M_i = T^2 / (T + A)^2, \quad (6)$$

where  $\delta m$  is the width of the interferometer instrumental function;  $R$  is the reflectance of the interferometer mirrors;  $K_i$  is the single-pass contrast;  $M_i$  is the interferometer transmittance;  $T$  and  $A$  are, respectively, the transmittance and the absorption coefficient of the interferometer mirrors.

The proposed monochromator is set in a Raman lidar either directly at the focal plane of the receiving antenna or at some distance from it. In the latter case, optical coupling with the use of optical wave guides is used. The needed matching is determined in the following way. Let us present the instrumental function of the interferometer  $\delta m$  in the form

$$\delta m = \delta \lambda / (\Delta \lambda) , \quad (7)$$

where  $\Delta \lambda$  is the FPI free spectral range;  $\delta \lambda$  is the instrumental function halfwidth. In our case,  $\delta \lambda$  is determined as spectral filling of the monochromator entrance slit.

For the proposed monochromator, the spectral filling  $\delta \lambda$  can be derived by differentiating Eq. (1) and excluding  $m$ :

$$\delta \lambda = \lambda \tan \varphi \delta \varphi , \quad (8)$$

where  $\delta \varphi$  is the angular width of the entrance aperture,

$$\delta \varphi = \frac{\cos^2 \varphi}{F} A_c . \quad (9)$$

The transmittance of the proposed monochromator  $M_m$  can be written in the form

$$M_m = M_{\text{lens}}^2 M_i^2 M_g , \quad (10)$$

where  $M_{\text{lens}}$  is the lens transmittance;  $M_g$  is the diffraction grating transmittance.

Suppression of the background level  $K_m$  in the monochromator is determined by the expression

$$K_m = K_i^2 K_g , \quad (11)$$

where  $K_g$  is the background suppression coefficient of the diffraction grating.

Let us consider a particular example to make clear the operating principle of the monochromator proposed. The lidar is assumed to operate (as in the most probable case) in the visible spectral region near  $0.532 \mu\text{m}$  being coupled with the monochromator through optical wave guides. Suppose that the wave guide diameter is  $0.3 \text{ mm}$ , the relative opening of the matched optical system is 1:3, and the interferometer clear aperture is  $50 \text{ mm}$ . Let us also assume that a  $600 \text{ grooves/mm}$  diffraction grating operates in the fifth order of diffraction. Then the focal length of the lens 3 is equal to  $150 \text{ mm}$ . The reciprocal linear dispersion of monochromator 4 in this case is  $13.5 \text{ \AA/mm}$ . The distance between the wave guides 2 and 4 (see Fig. 2), equals to  $3.77 \text{ mm}$ , that causes the smallest diameter of circle 5 and the angle  $\varphi = 0.72^\circ$ . Calculating the separation, specular reflectance, and single-pass contrast for the interferometer by Eqs. (1) and (4)–(9), we obtain  $d = 0.6282 \text{ mm}$ ,  $R = 0.834$ ,  $K = 122$ . Thus, for a double passage optical arrangement, the suppression of the on-line scattered radiation (wave guide 3) by the interferometer is of the order of  $10^{-4}$ . For the wave guides 2 and 4, the diffraction grating contributes additional suppression of the order of  $10^{-4}$ , so the total value is as low as  $10^{-8}$ .

If an interferometer is set in front of the monochromator, following the traditional scheme, then the above example demonstrates low, only of the order of  $10^2$ , single-pass contrast for the interferometer. Such a value is governed by the conditions of matching between the parameters of the interferometer and the lidar receiving antenna for the most widely accepted case.

The proposed monochromator solves this problem optimally.

To prove the validity of the proposed design in comparison with the double monochromator, consider the parameter

$$\gamma = P \delta \lambda / K , \quad (12)$$

where  $P$  is the power received at the sounding radiation wavelength;  $K$  is the coefficient of the on-line scattering suppression in an adjacent spectral region.

Thus,  $\gamma$  can be considered as a characteristic of background radiation coming to a receiver. For the double monochromator with the diffraction grating, the spectral filling of the entrance slit is usually chosen about  $10 \text{ \AA}$  at the suppression of  $10^{-8}$ .

For the considered case  $\delta \lambda = 0.13 \text{ \AA}$  at the suppression of  $10^{-8}$ . Thus, the ratio between the characteristics  $\gamma$  of both monochromators is 1:77, what clearly counts in favor of the proposed monochromator design.

Besides, separation of the rotational spectral structure of the gaseous atmospheric constituents of

interest under conditions of atmospheric pollution is a positive factor.

I recommend to use the optical arrangement shown in Fig. 3 for the proposed monochromator design. A spherical or, what's better, parabolic mirror is used here instead of the lens. Arrangement of entrance and exit wave guides in the image plane (see Fig. 2) remains the same.

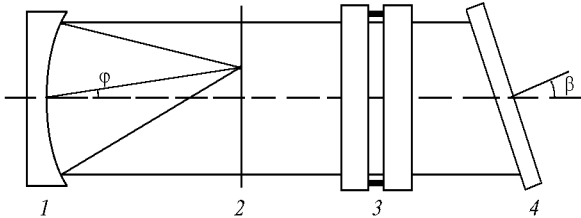


**Fig. 3.** The proposed design of the monochromator: a spherical mirror (1), the entrance/exit plane (2), a Fabry-Perot interferometer (3), a diffraction grating (4).

In this case, the background radiation incident on the receiving optical wave guides 2 and 4 (this radiation appears from scattering at optical parts) does not contain the part of radiation, which was reflected at refraction on the lens. It is an important point to be noted.

The background radiation at the receiving light guides consists of (in the descending order) sparkles reflected at refraction on optical parts, radiation scattered on dust and construction elements, and diffraction effects on the emitting wave guides.

A spot from antireflection coating of the lens, while being incident onto the light guide receiving plane, contributes about 0.1% into the total power of radiation coming to the monochromator. Then, at the wave guide cross section of  $0.1 \text{ mm}^2$  and the spot diameters about 30 mm, the background can contribute up to  $10^{-5}$  of the total power of radiation at the light guide.

Dusted optical surfaces contributing into the background radiation can be considered as screens that scatter in all directions. The background level of  $10^{-8}$  at the receiving light guides means that the scattered power makes up from 0.5 to 1%, what can be evaluated as a greater-than-average dust level.

The influence of background from diffraction effects on wave guide 1 or 6 on the wave guides 2 and 4 in this case can contribute<sup>6</sup> no more than  $10^{-9}$ – $10^{-10}$  of the total radiation power, taking into account the

wave guide arrangement and the fact that the wave guide diameter far exceeds the wavelength.

A conclusion can be drawn that with perfect manufacture the mirror version of the proposed monochromator is preferable. The proposed monochromator has small size and use a smaller number of optical elements than the double monochromator. As compared to the two-beam monochromator,<sup>7</sup> it does not need a communication unit of wave guides.

Manufacture of an intermediate ring for the interferometer is not problematic, because its width may vary in some range, thus defining the diameter of circle 5 in the image plane. Circle 5, in its turn, specifies the arrangement of wave guides 2 and 4, which depends also on the parameters of the mirror and the diffraction grating used. The wave guide unit is manufactured with a fixed arrangement of the wave guides. The interferometer and diffraction grating are mounted in the adjustment holders. Adjustment of the monochromator is rather easy and consists of two stages. The sensing laser radiation is directed onto the entrance optical wave guide 1, and the interferometer is aligned so that the radiation reflected from it as a result of interference comes to the wave guide 6. Then, at the second stage, the diffraction grating is adjusted so that the attenuated laser radiation is collected by the wave guide 3.

We can assume that at perfect manufacture the proposed result will satisfy the requirements of high spectral selectivity, close matching with the lidar, and small size.

## References

1. J.J. Barrett and S.A. Mayers, *J. Opt. Soc. Am.* **61**, No. 9, 1246–1251 (1971).
2. W.S. Hayden, *Opto-Spectr.* **4**, No. 2, 161–167 (1972).
3. J.J. Barrett, in: *Laser Raman Gas Diagnostics*, M. Lapp and C.M. Penney, eds. (Plenum Press, New York, 1974), pp. 63–85.
4. A. Cohen, J.A. Cooney, and K.N. Geller, *Appl. Opt.* **15**, No. 11, 2896 (1976).
5. M.M. Sushchinskii, *Raman Spectra of Molecules and Crystals* (Nauka, Moscow, 1967), 548 pp.
6. S. Solimeno, B. Krozinyani, and P. De Porto, *Diffraction and Wave-Guide Propagation of Optical Radiation* [Russian translation] (Mir, Moscow, 1989), 664 pp.
7. S.N. Volkov, B.V. Kaul', V.A. Shapranov, and D.I. Shelefontyuk, *Atmos. Oceanic Opt.* **8**, No. 10, 833–835 (1995).